Simple Embossing Process for Fabricating GMR Biosensor with Variable waveguide Thickness

Ting-Jou Ding, Jiann-Hwa Lue, Tsung-Hsun Yang*

Department of Optics and photonics, National Central University, Chungli, Taiwan, ROC
thyang@dop.ncu.edu.tw

Abstract: This work demonstrates a simple fabrication process for the guided-mode resonance biosensors with tunable waveguide thickness. For various waveguide thicknesses, the grating parameters can still keep the same. Although consisted of the waveguide layer and the grating layer, the GMR biosensor can be simply fabricated in a single step and of the same material by the conventional embossing technique. Moreover, the thickness of waveguide can be well controlled by applying various forces. It is shown that the tunable range of the waveguide thickness is approximately to 600nm and the deformation on the grating layer still keeps less than 10%.
[Ting-Jou Ding, Jiann-Hwa Lue, Tsung-Hsun Yang. **Simple Embossing Process for Fabricating GMR Biosensor with Variable waveguide Thickness**. Life Sci J 2012;9(2):1020-1026] (ISSN:1097-8135). http://www.lifesciencesite.com. 152

Keywords: soft lithography; spin-on glass; grating; waveguide; subwavelength; embossing

1. Introduction

The guided-mode resonance (GMR) sensor as one of the optical biosensor has presented several advantages including: (i) monitoring in real time, (ii) labeled-free detection to simplify assay, (iii) less analysis time, (iv) high potential for high throughput device, and (v) compact measurement system[1-9].

For the consideration of low cost and high throughput, simple and easy-made structure has more advantages in practical applications. In the construction of GMR sensor, it simply consists of one sub-wavelength diffraction grating and one waveguide layer. Figure 1 illustrates the schematic structure of GMR sensor. In the figure 1, the structure of GMR sensor can be subdivided into several parts: period, filling factor, grating depth, and waveguide thickness.

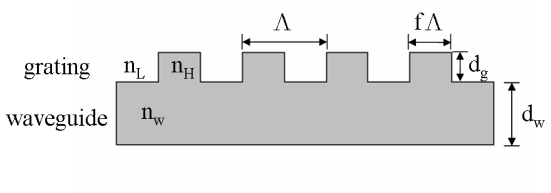

Figure 1. The schematic structure of GMR sensor. The GMR sensor, it simply consists of one sub-wavelength diffraction grating and one waveguide layer. It can be subdivided into several parts: period, filling factor, grating depth, and waveguide thickness in detail.

As being an excellent sensor, the capacity of high throughput in fabrication is an important factor. However, the conventional fabricating methods for GMR sensor can be sorted roughly by lithography and imprint techniques [10-15]. In the sub-micro or nanometer scale applications, conventional lithography techniques require more expensive equipments to increase resolution. For the high throughput fabrication objective, it is a major issue under the consideration of cost and commerce.

On the other hand, imprint techniques don't need expensive equipments in high throughput fabrication but have simple fabricating processes instead. Imprint techniques provide a powerful tool in micro and nanometer scale applications. Fabricating GMR sensor by nanoimprint is an excellent solution for low cost and high throughput consideration. In the conventional nanoimprint, a "hard" material, usually silicon, or glass based, is used to be the master mold. Generally, this master mold transfers designed patterns to UV-curing or heat-curing material. After stripping the mold, a high refractive index (or dielectric constant) layer was deposited on curing material to form GMR sensor. In general, low refractive index curing materials and high refractive index deposited layer are usually chosen to enhance the sensitivity. This method provides a cheap and powerful solution in nanofabricating. However, imprinting step in this fabricating process only defines and transfers patterns to curing materials. Nanoimprint does not build the GMR sensor. The higher refractive index deposited layer constructs GMR sensor's main structure after depositing step. In this method, two-step fabricating processes have room for improvement. If nanoimprint is the only needed fabricating process, the fabrication will not only be more efficient but cost less. For fabricating GMR sensor, simpler fabricating processes development is an important and attractive issue.

Soft lithography is a new concept in nanoimprint field [16-22]. The greatest feature of soft lithography is using an elastomer as a mold, a stamp,

or a mask. The elastomer mold replaces the rigid ones and is used to transfer designed patterns. Comparing to conventional imprint techniques, the soft mold is capable of larger-sized imprinting, such as tens centimeter-scale. Moreover, it has superiority in imprinting two-dimension and three-dimension structures [16]. Soft lithography technology approximately includes microcontact printing (μCP)[19,23-25], replica molding (REM)[26-27], microtransfer molding (μTM)[19,28], micromolding in capillaries (MIMIC)[29-31], embossing[32-33]. For the fabrication of GMR sensor by soft lithography, Magnusson fabricates GMR sensor by micromolding in capillaries (MIMIC) [34]. In their fabricating steps, GMR sensor was divided into two parts, grating and waveguide fabrications. The waveguide part was first deposited on the substrate with a high refractive index layer. Then, the grating part was formed by the micromolding in capillaries (MIMIC). In this method, the waveguide thickness is adjustable depending on the depositing thickness and not controlled by imprint step. It is a useful experimental design because the adjustable waveguide thickness is a key factor to GMR sensor. The thickness of waveguide has great influence on sensitivity. MIMIC technique is a powerful protocol in nanoimprint but has several limitations for GMR sensor fabrication. In MIMIC, the capillaries are the domain force to make the imprint materials fill into whole patterns. It needs much more time when the imprinting area increases. Embossing, one of soft lithography technology, has great superiority in GMR sensor fabrication. The outstanding characteristics of embossing are include a single procedure and high throughput. Embossing also makes the waveguide thickness adjustment possible due to its intrinsic properties.

In our work, we developed a cheap and stable imprint system to realize the fast fabrication of GMR sensor. This cheap imprint system only cost about 400 dollars. Utilizing this imprint system, we demonstrated a single procedure method successfully for fabricating adjustable waveguide thickness GMR sensor by embossing technique. In the practical fabrication, the liquid spin-on glass (SOG) was used as imprinting material.

2. Soft Lithography Process

Elastomer mold: Polydimethyl siloxane (PDMS) is the major material used as an elastomer. In the elastomer mold constituent, SylgardR 184 silicone elastomer from Dow Corning was used. The characteristic of low surface energy makes mold stripping easily without any released agents.

Pattern material: In this experiment, the material to pattern is Spin-on glass (SOG). SOG is a mixture of SiO_2 and dopants suspending in a solvent solution. We use SOG (IC1-200) containing 7.2% solids content from Futurrex.

Figure 2 shows the schematic fabrication process of GMR sensor by the embossing technique. The waveguide and grating of GMR sensor were produced at the same in imprinting step.

(a) Prepare Si master template.

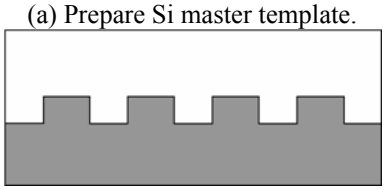

(b) Apply and cure PDMS and Remove Si master template.

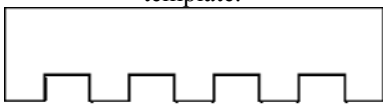

(c) PDMS mold.

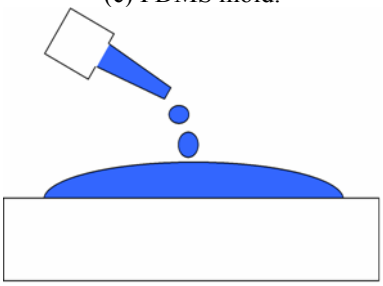

(d) Apply liquid SOG solution on a ITO glass substrate.

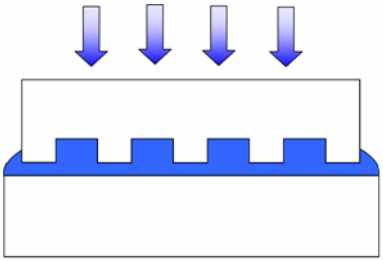

(e) Press PDMS mold on and heat. Then, Stripping PDMS mold.

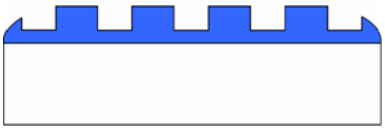

(f) Fabricated element.

Figure 2. Scheme of the fabrication processes for producing one-dimension grating and waveguide structure by embossing. The elastomer mold production and imprint procedure composes of the whole processes.

In the beginning of procedures, a patterned silicon plate is prepared as the master template. This template was patterned of some sub-wavelength gratings by conventional e-beam lithography. The pattern size of sub-wavelength grating is 2 mm^2. Next, transfer the patterns and structures from the template to the elastomer PDMS mold. The SylgardR 184 silicone elastomer was mixed with the curing agent of 10:1 ratio by weight and standing until the air bubbles escaped from mixture. Applying PDMS on the template and heating 10 minutes at 100°C to cure PDMS. After curing step, the PDMS mold was stripped from silicon template. This PDMS mold plays an important role in embossing soft lithography. PDMS mold was taken as major mold replacing of rigid silicon template in soft lithography technology. In the imprint steps, the SOG liquid was applied on the surface of the glass substrate and pressed with PDMS mold. After impression step, the imprint stage heated from the room temperature to 90°C and made the solvent vapor. Two hours later, the PDMS mold was stripped from glass substrate.

This imprint method is not only designed for GMR sensor fabrication but also capable of two-dimension arbitrary patterns transference and adjustable waveguide thickness fabrication. Figure 3 shows the SEM pictures of one-dimension grating and two-dimension microcaves fabricated at 90°C with 24.8N output force.

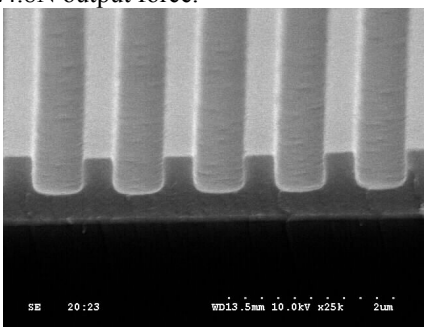

(a)

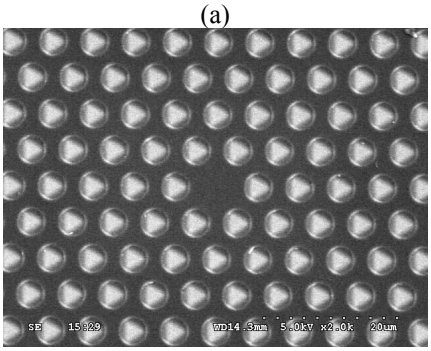

(b)

Figure 3. The SEM pictures of (a)one-dimension grating and (b)two-dimension microcaves. Both of them were fabricated at 90°C with 24.8N output force.

In our experiment setup, the size of the PDMS mold is 1cm×1.3cm and the volume of SOG solution is 6 microliter. As maintaining at 90°C, the output force from the pressure cylinder was set approximately to 3.4N, 24.8N, 37.5N, and 50.2N, respectively.

3. Instruments and Setup

We develop an imprint system to fabricate waveguide thickness adjustable GMR sensor by embossing technique. Figure 4 shows the construction of the major imprint device. It is composed of several parts: frames, heaters, thermal sensors, thermal insulators, pressure cylinder, air valve controller, imprint stage, leveling adjustment components, and a plastic cover box. The heaters, thermal sensors, and the thermal insulators construct temperature control system. It provides stable and controllable surrounding temperature. In this temperature control system, power supply provides all the needed energy. The pressure cylinder and air valve controller provide the controllable output force in the imprinting processes. The outside cover prevents the disturbance of heat convention and helps to keep surrounding temperature stable.

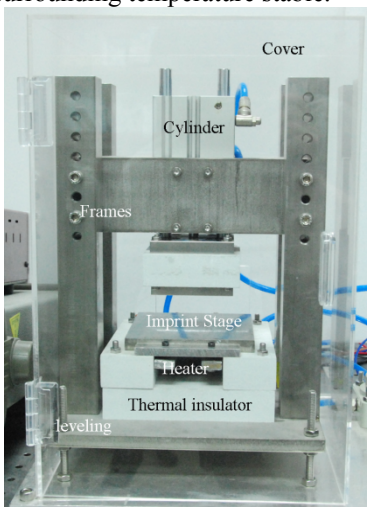

Figure 4. The picture of imprint device which is the major part included in self-developed imprint system. This imprint device composes of several parts including stainless frames, heater, thermal sensor, thermal insulator, pressure cylinder, air valve controller, imprint stage, leveling adjustment components, and a plastic cover preventing the disturbance of any airflow.

Figure 5 show the self-developed imprint system. This imprint system is composed of major imprint device, temperature control system, power supply, and pressure control system. For the low cost consideration, it costs only approximately 400 dollars

expect power supply. Simple construction makes assembly and operation easier. In this self-developed imprint system, low cost, stable, and practical are the notable characteristics of our design. This imprint system provides heating range from room temperature to 160°C and pressing force approximately up to 78 N.

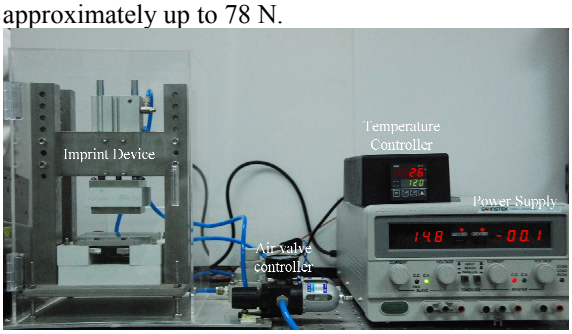

Figure 5. The picture of self-developed imprint system. This imprint system includes major imprint device, pressure controller system, temperature controller system, and power supply. The whole imprimt, expect the power supply, costs approximately 400 dollars. It is a cheap, stable, and practical design for imprinting.

4. Characterization

Embossing technique has two key factors, heating temperature and pressure (or output force) during the fabricating processes. In the functionality considerations, heating mainly evaporates solvent of imprinting material. The total amount of solutes in liquid imprinting material has small variation during the heating process. Heating only influences the evaporator rates but changes the total amount of solutes. The higher temperature makes faster evaporator. The experimental result of different heating temperature at constant press force (50.2N) condition shows in figure 6. In figure 6, the waveguide thickness keeps approximately in the order of 100 nm from room temperature to 120°C.

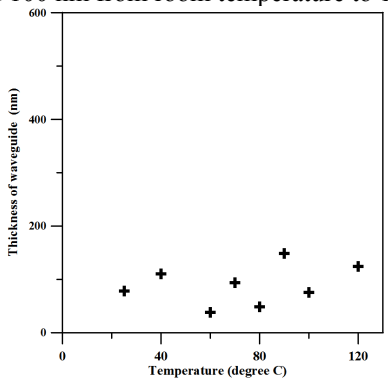

Figure 6. The variation of waveguide thickness at different temperature. The temperature range is form room temperature to 120°C and the output force in all cases is 50.2N.

5. Results and Discussion

Figure 7 shows the scanning electron microscope (SEM) picture of silicon template in top view. The grating period of this template is 1,013 nm and the filling factor is approximately 0.4. The grating depth is 520nm.

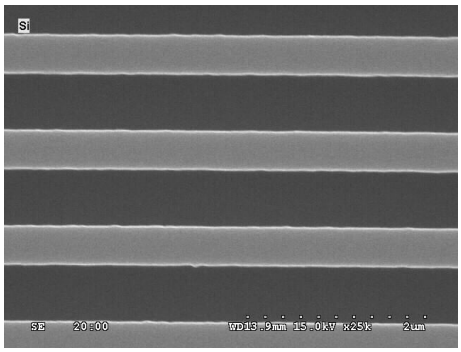

(a)

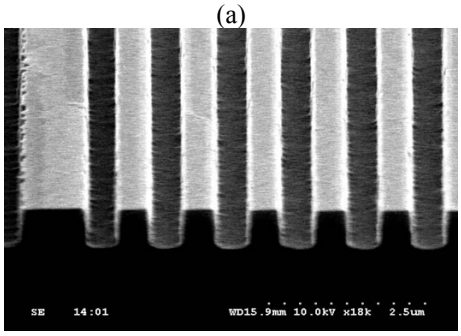

(b)

Figure 7. Scanning electron microscope (SEM) picture of silicon template in top view (a) and side view (b). The grating period of this template is 1013nm and the filling factor is approximately 0.4. The grating depth is 520nm.

Figure 8 shows the SEM pictures of each one-dimension grating and waveguide structure fabricating under different compressed force conditions at 90°C.

In those pictures, the thickness of waveguide decreases with the increments of compressed force. Those pictures also show that the characteristics of grating have less variation than thickness of waveguide. The variations of the period, the depth, and the filling factor of the grating are all less than 10%. It reveals that the grating characteristics have been reproduced very well.

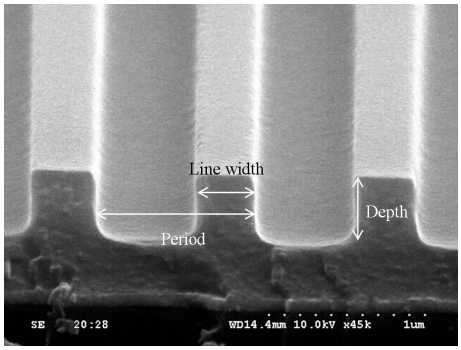

Figure 8. SEM pictures of one-dimension grating and waveguide structure fabricating under different compressed force conditions at 90°C. The picture of output force shows (b) 24.8N.

Figure 9 shows the relationship of output force and thickness of waveguide. Without doubts, the larger the output force is, the thinner the waveguide layer of the grating is. In the range of applicable force, the thickness of the waveguide layer of the grating reduces 10 nm per N pressing force.

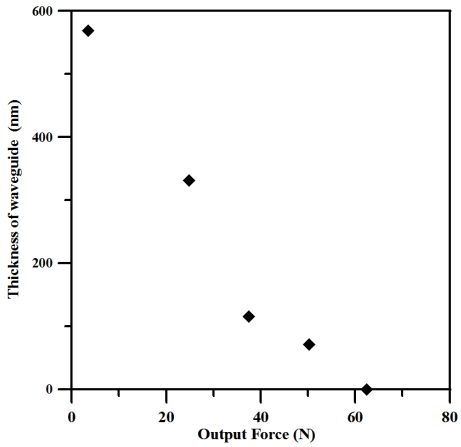

Figure 9. Relation between the output force and the resulting thickness of waveguide. The resulting thickness of the waveguide is inversely proportional to the output force.

Figure 10 shows the shrinkage between imprint sample and silicon mold. The graph shows the shrinkage rates of grating depth, line width, and period. In this case, the shrinkage rates of depth, line width and period are approximately 31.2, 10.5 and 3.2 respectively.

In the design of this experiment, the solvent vaporization time was set up to two hours which is enough for entire formation. This solvent vaporization time relies on the intrinsic characteristics of solvent. For our used SOG type, this time can reduce to 10 minutes in the condition of 24.8N applied force and 90°C.

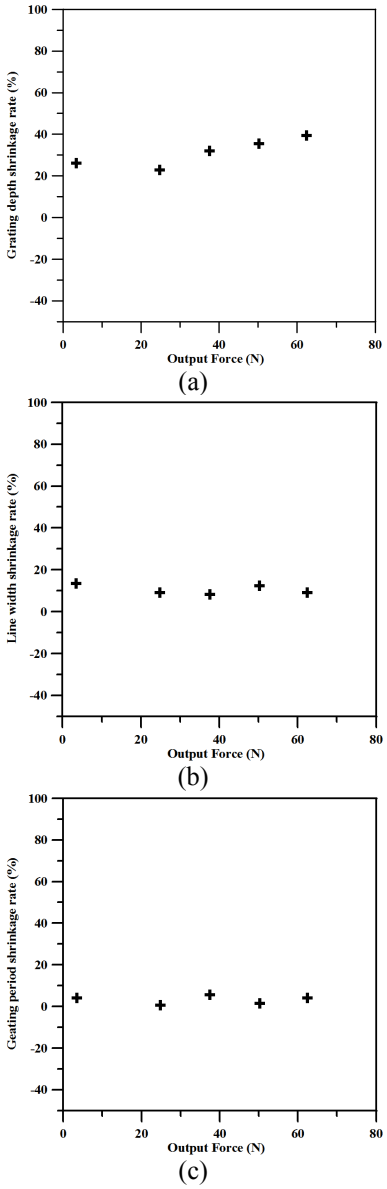

Figure 10. Shrinkage rates of (a) grating depth (b) grating line width (c) grating period versus the output force. In this case, the shrinkage rates of grating depth, line width and period are around 31.2, 10.5 and 3.2, respectively.

6. Conclusions

In conclusion, we present a method for fabricating adjustable waveguide thickness guided-mode resonance (GMR) biosensor successfully. The waveguide and grating can be fabricated in a single step and of the same material, spin-on glass (SOG), by embossing technique. In our case, the adjustable waveguide thickness range is around 600nm and the grating deformation can still keep less than 10%. For GMR biosensor design and fabrication, the stable grating structure and changeable waveguide thickness

make the design into reality easier. The short formation time also helps to achieve low cost and high throughput objective easily.

Acknowledgments
This wok was partly sponsored by the National Science Council, Taiwan, under the grant numbers of NSC 101-3113-E-008-001 and NSC 101-2911-I-008-501, and also partly sponsored by National Central University, Taiwan, under the grant number of 101G903-2.

Corresponding Author:
Tsung-Hsun Yang, Ph.D.
Department of Optics and photonics, National Central University, Chungli, Taiwan, ROC
No. 300, Jhongda Rd., Jhongli City, Taoyuan County 32001, Taiwan, ROC
E-mail: thyang@dop.ncu.edu.tw

References

1. S. S. Wang, R. Magnusson. (1992) New principle for optical filters. Appl. Phys. Lett.. 61: 1022-1024.
2. S. S. Wang, R. Magnusson. (1993) Theory and applications of guided-mode resonance filters. Appl. Opt.. 32: 2606-2613.
3. S. S. Wang, R. Magnusson, J. S. Bagby, M. G. Moharam. (1990) Guided-mode resonances in planar dielectric-layer diffraction gratings. J. Opt. Soc. Am.. 7: 1470-1474.
4. Brian Cunningham, Bo Lin, Jean Qiu, Peter Li, Jane Pepper, Brenda Hugh. (2002) A plastic colorimetric resonant optical biosensor for multiparallel detection of label-free biochemical interactions. Sensors and Actuators B. 85: 219-226.
5. Carlos F. R. Mateus, Michael C. Y. Huang, Peter Li, Brian T. Cunningham, Connie J. Chang-Hasnain. (2004) Compact Label-Free Biosensor Using VCSEL-Based Measurement System, IEEE Photonics Technology Letters. 16: 1712-1714.
6. J. N. Yih, Y. M. Chu, Y. C. Mao, W. H. Wang, F. C.Chien, C. Y. Lin, K. L. Lee, P. K. Wei, S. J. Chen. (2006) Optical waveguide biosensors constructed with subwavelength gratings. Appl. Opt.. 45: 1938-1942.
7. Bo Lin, Peter Li, Brian T. Cunningham. (2006) A Label-free biosensor-based cell attachment assay for characterization of cell surface molecules. Sensor and Actuators B. 114: 559-564.
8. Dennis W. Dobbs, Irena Gershkovich, Brian T. Cunningham. (2006) Fabrication of a graded-wavelength guided-mode resonance filter photonic crystal. Applied Physics Letters. 89: 1123113.
9. Charles J. Choi, Brian T. Cunningham. (2007) A 96-well microplate incorporating a replica molded microfluidic network integrated with photonic crystal biosensors for high throughput kinetic biomolecular interaction analysis. Lab on a chip. 7: 550-556.
10. J. T. M. Stevenson, A. M. Gundlach. (1986) The Application of Photolithography to the Fabrication of Microcircuits. Journal of Physics E-Scientific Instruments. 19: 654-667.
11. C. H. Ting, M. Hatzakis, R. A. Leone. (1975) Fabrication of Microelectronic Devices with Electron-Beam Lithography. Journal of Vacuum Science & Technology. 12: 1304-1304.
12. H. Ahmed. (1976) Electron-Beam Lithography for Microcircuit Fabrication. Electronics and Power. 22: 433-436.
13. S. V. Springham, T. Osipowicz, J. L. Sanchez, L. H. Gan, F. Watt. (1997) Micromachining using deep ion beam lithography. Nucl. Instrum. Methods Phys. Res. Sect. B-Beam Interact. Mater. Atoms. 130: 155-159.
14. J. Jonkers, (2006) High power extreme ultra-violet (EUV) light sources for future lithography. Plasma Sources Sci. Technol. 15: S8-S16.
15. Stephen Y. Chou, Peter R. Krauss. (1996) Imprint lithography with 25-nanometer resolution. Science. 272: 85-87.
16. P. D. Yang, G. Wirnsberger, H. C. Huang, S. R. Cordero, M. D. McGehee, B. Scott, T. Deng, G. M. Whitesides, B. F. Chmelka, S. K. Buratto, G. D. Stucky. (2000) Mirrorless lasing from mesostructured waveguides patterned by soft lithography. Science. 287: 465-467.
17. J. P. Rolland, E. C. Hagberg, G. M. Denison, K. R. Carter, J. M. De Simone. (2004) High-resolution soft lithography： Enabling materials for nanotechnologies. Angew. Chem.-Int. Edit. 43: 5796-5799.
18. D. Qin, Y. N. Xia, G. M. Whitesides. (2010) Soft lithography for micro- and nanoscale patterning. Nat. Protoc. 5: 491-502.
19. X. M. Zhao, Xia Y, G. M. Whitesides. (1997) Soft lithographic methods for nano-fabrication. Journal of Materials Chemistry. 7: 1069-1074.
20. Marc A. Unger, Hou-Pu Chou, Todd Thorsen, Axel Scherer, Stephen R. Quake. (2000) Monolithic Microfabricated Valves and Pumps by Multilayer Soft Lithography. Science. 288: 113-116.
21. Peidong Yang, Gernot Wirnsberger, Howard C. Huang, Steven R. Cordero, Michael D. McGehee, Brain Scott, Tao Deng, George M. Whitesides, Bradley F. Chmelka, Steven K. Buratto, Galen D.

Stucky. (2000) Mirrorless Lasing from Mesostructured Waveguides Patterned by Soft Lithography. Science. 287: 465-467.
22. Xiao-Mei Zhao, Younan Xia, George M. Whitesides. (1997) soft lithographic methods for nanofabrication. J. Mater. Chem. 7: 1069-1074.
23. Bernard A, Renault JP, Michel B, Bosshard HR, Delamarche E. (2000) Microcontact Printing of Proteins. Adv. Mater. 12: 1067-1070.
24. James L. Wilbur, Amit Kumar, Enoch Kim, George M. Whitesides. (1994) Microfabrication by microcontact printing of self-assembled monolayers. Adv. Mater. 6: 600-604.
25. Amit Kumar, Nicholas L. Abbott, Hans A. Biebuyck, Enoch Kim, George M. Whitesides. (1995) Patterned self-assembled monolayers and meso-scale phenomena. Acc. Chem. Res. 28: 219-226.
26. Younan Xia, Enoch Kim, Xiao-Mei Zhao, John A. Rogers, Mara Prentiss, George M. Whitesides. (1996) Complex Optical Surfaces Formed by Replica Molding Against Elastomeric Masters. Science. 273: 347-349.
27. Younan Xia, Jabez J. McClell, Rajeev Gupta, Dong Qin, Xiao-Mei Zhao, Lydia L. Sohn, Robert J. Celotta, George M. Whitesides. (1997) Replica molding using polymeric materials: A practical step toward nanomanufacturing. Adv. Mater. 9: 147-149.
28. Xiao-Mei Zhao, Younan Xia, George M. Whitesides. (1996) Fabrication of three-dimensional micro-structures: Microtransfer molding. Adv. Mater. 8: 837-840.
29. KIM E., YOUNAN XIA, WHITESIDES G. M. (1995) Polymer microstructures formed by moulding in capillaries. Nature. 376: 581-584.
30. Younan Xia, Enoch Kim, George M. Whitesides, (1996) Micromolding of polymers in capillaries: applications in microfabrication. Chem. Mater. 8: 1558-1567.
31. Enoch Kim, Younan Xia, George M. Whitesides. (1996) Micromolding in Capillaries: Applications in Materials Science. J. Am. Chem. Soc. 118: 5722-5731.
32. Colin A. Bulthaup, Eric J. Wilhelm, Brian N. Hubert, Brent A. Ridley, Joseph M. Jacobson. (2001) All-additive fabrication of inorganic logic elements by liquid embossing. Appl. Phys. Lett. 79: 1525-1527.
33. Eric J. Wilhelm, Joseph M. Jacobson. (2004) Direct printing of nanoparticles and spin-on-glasses by offset liquid embossing. Appl. Phys. Lett. 84: 3507-3509.
34. Lee, K. J., J. Jin, Byeong-Soo Bae, Robert Magnusson. (2009) Optical filters fabricated in hybrimer media with soft lithography. Opt Lett. 34: 2510-2512.

5/22/2012